

# Amplify Adjacent Token Differences: Enhancing Long Chain-of-Thought Reasoning with Shift-FFN

Yao Xu<sup>1,2,5</sup>, Mingyu Xu<sup>3</sup>, Fangyu Lei<sup>1,2</sup>, Wangtao Sun<sup>1,2</sup>, Xiangrong Zeng<sup>3</sup>,  
Bingning Wang<sup>3</sup>, Guang Liu<sup>5</sup>, Shizhu He<sup>1,2</sup>, Jun Zhao<sup>1,2</sup>, Kang Liu<sup>1,2,4\*</sup>

<sup>1</sup> The Laboratory of Cognition and Decision Intelligence for Complex Systems,  
Institute of Automation, Chinese Academy of Sciences, Beijing, China

<sup>2</sup> School of Artificial Intelligence, University of Chinese Academy of Sciences, Beijing, China

<sup>3</sup> Baichuan Inc, Beijing, China

<sup>4</sup> Shanghai Artificial Intelligence Laboratory, Shanghai, China

<sup>5</sup> Beijing Academy of Artificial Intelligence, Beijing, China

{yao.xu, shizhu.he, jzhao, kliu}@nlpr.ia.ac.cn

## Abstract

Recently, models such as OpenAI-o1 and DeepSeek-R1 have demonstrated remarkable performance on complex reasoning tasks through Long Chain-of-Thought (Long-CoT) reasoning. Although distilling this capability into student models significantly enhances their performance, this paper finds that fine-tuning LLMs with full parameters or LoRA with a low rank on long CoT data often leads to *Cyclical Reasoning*, where models repeatedly reiterate previous inference steps until the maximum length limit. Further analysis reveals that smaller differences in representations between adjacent tokens correlates with a higher tendency toward *Cyclical Reasoning*. To mitigate this issue, this paper proposes Shift Feedforward Networks (Shift-FFN), a novel approach that edits the current token’s representation with the previous one before inputting it to FFN. This architecture dynamically amplifies the representation differences between adjacent tokens. Extensive experiments on multiple mathematical reasoning tasks demonstrate that LoRA combined with Shift-FFN achieves higher accuracy and a lower rate of *Cyclical Reasoning* across various data sizes compared to full fine-tuning and standard LoRA. Our data and code are available at <https://anonymous.4open.science/r/Shift-FFN>.

## 1 Introduction

In recent years, Large Reasoning Models (LRMs) such as OpenAI-o1 [13], DeepSeek-R1[3], and Qwen3 [43] have achieved significant advancements in mathematical, coding, and other complex reasoning tasks. A key factor behind their success lies in extending the traditional Chain-of-Thought (CoT) [37] approach into long CoT, which incorporates detailed step-by-step reasoning, multiple solution strategies and self-reflection processes [1].

Long Chain-of-Thought (CoT) demonstrates remarkable reasoning abilities, but training language models to exhibit such complex reasoning requires substantial computational resources. Consequently, knowledge distillation [42, 44, 15, 23] has emerged as a prevalent approach to impart this extended reasoning capabilities to smaller models by training them on instruction-response instances enriched with short/long CoT (short/long CoT datasets for short). Therefore, how to enable student models to effectively learn from these long CoT datasets has emerged as a fundamental scientific problem.

---

\* Corresponding Author

One potential method could be Parameter-Efficient Fine-Tuning (PEFT) [7] such as LoRA [12], which achieves performance comparable to full fine-tuning on several tasks such as commonsense reasoning [2], and instruction following [18], despite updating only a minimal subset of parameters. However, these tasks typically do not involve long CoT reasoning and generally maintain output lengths within only 1k tokens, whereas long CoT data frequently exceed 16k tokens. This discrepancy naturally raises a critical research question: **Is the PEFT approach still effective when applied to learning long CoT reasoning?**

This paper first investigates this question by constructing parallel datasets containing short CoT and long CoT solutions for identical questions, respectively. The short and long CoT datasets are sourced from Numina Math dataset [16] and DeepSeek-R1 outputs, respectively. Two student models are trained separately using LoRA [12] and full fine-tuning, respectively. This paper observes that with a rank of 32, LoRA achieves comparable performance to full fine-tuning on short CoT dataset. However, a noticeable performance gap emerges between LoRA and full fine-tuning in long CoT scenarios, as shown in Figure 1 (left). This paper finds that both LoRA and full fine-tuned models tend to exhibit *Cyclical Reasoning*, where they repeatedly generate paragraphs or reiterate previous inference steps until reaching the maximum length limit of 32k tokens, Figure 1 (right). This phenomenon is more pronounced in LoRA with lower rank, contributing to the performance gap compared to full fine-tuning. Further analysis reveals that low divergence of adjacent tokens correlates with a higher tendency toward *Cyclical Reasoning*. Specifically, this paper finds that: (1) For the same model, answers exhibiting *Cyclical Reasoning* show smaller internal representation differences between adjacent tokens compared to normal answers. (2) For LoRA fine-tuned models, a higher rank reduces the rate of *Cyclical Reasoning* while simultaneously increases the internal representation differences between adjacent tokens (more details in Section 3.1).

Based on these observations, the paper proposes Shift Feedforward Network (Shift-FFN), which introduces an Editor module before the FFN. The Editor module uses the preceding token’s representation to edit the current token’s representation, thereby dynamically amplifying the representation differences between adjacent tokens within the model, as shown in Figure 3. Experimental results demonstrate that LoRA combined with Shift-FFN achieves higher accuracy and a lower rate of *Cyclical Reasoning* across various data sizes compared to full fine-tuning and standard LoRA.

The main contributions of this work are as follows:

1. This paper finds that fine-tuning LLMs with full parameters or LoRA with a low rank on long CoT data often leads to *Cyclical Reasoning*, and observes smaller differences in representations between adjacent tokens correlates with a higher tendency toward *Cyclical Reasoning*.
2. This paper proposes Shift-FFN, which edits the current token’s representation with the previous one before FFN, thereby dynamically amplifying differences between adjacent tokens.
3. Experimental results show that introducing Shift-FFN into LoRA improves model accuracy and reduces the ratio of *Cyclical Reasoning*.

## 2 Related Work

**Parameter-Efficient Fine-Tuning methods (PEFTs).** PEFT methods adapt models to downstream tasks by updating only a small subset of parameters. Existing PEFT methods can be categorized into the following three categories [7]:

1. **Addition based methods** train additional lightweight modules that are positioned within the frozen model. Adapters insert small adapter layers between LM attention or MLP layers [11, 34, 9]. Prompt tuning inserts randomly-initialized soft tokens at the beginning of the input texts and trains their embeddings while keeping the LM weights frozen [14, 17].
2. **LoRA** [12] and its variants [46, 21] employ low-rank matrix approximations for weight updates during training, while introducing no inference overhead as the updates can be directly merged into the base model parameters.
3. **Representation editing based methods** are motivated by representation engineering which demonstrates that adding "steering vectors" to the representation of each hidden layer can control pretrained LM generations [28, 20, 31]. Therefore, these methods learn to modify the hidden representations generated by multi-head attentions or FFNs [22, 39, 40]

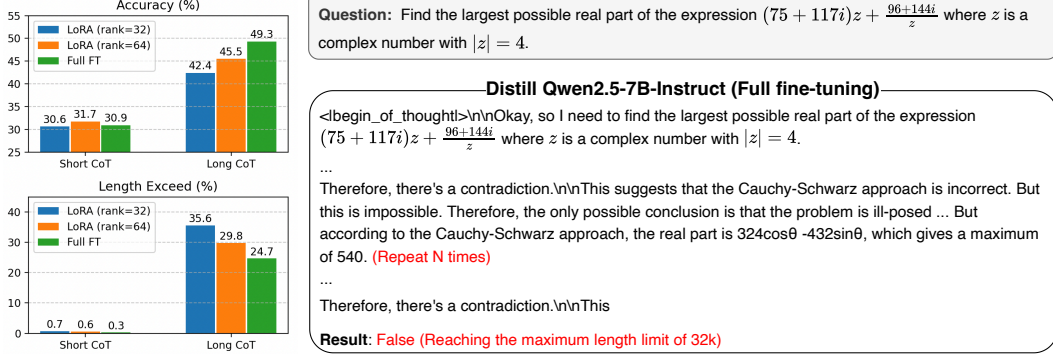


Figure 1: (Left), performance comparison of LoRA and Full Fine-Tuning (Full FT) on Accuracy (%) and Length Exceed (%) metrics for short CoT and long CoT datasets. "Accuracy" represents the average accuracy across four mathematical tasks. "Length Exceed" indicates the percentage of model outputs that exceed the maximum length limit. (Right), an example of *Cyclical Reasoning*.

Our proposed Shift-FFN can be viewed as a representation editing-based method, but it incorporates preceding token information in the updating of representation.

**Long CoT Distillation.** Extensive studies have demonstrated that distilling long CoT data from powerful reasoning models into student models can significantly enhance the students' reasoning capabilities [3, 43, 38]. Furthermore, LIMO [44] reveals that a small set of carefully selected examples suffices to elicit the model's complex mathematical reasoning capabilities. [15] finds that the structure of long CoT proves essential for effective learning, while the specific content within individual reasoning steps exhibits minimal impact. DLCoT [23] proposes to optimize long CoT through segmentation, redundancy elimination, and error correction. Their experimental results demonstrated that eliminating redundant reasoning paths leads to improvements in distillation efficiency. While existing approaches primarily investigate from a data perspective, this paper focuses on model architecture, enabling Shift-FFN to be complementary with such methods.

**Token Shift.** RWKV [24] introduces time-mixing and channel-mixing by computing linear projections from weighted combinations of the current and previous input representations within each block. KV shift [41] performs linear combinations of the current token's key/value vectors with those of the preceding token, and demonstrates that Shift-KV attention exhibits enhanced capability in learning induction heads. Fox [19] dynamically computes the weighting coefficient for the preceding token in the shift operation, followed by RMSNorm (Root Mean Square Normalization) [45] of the weighted results. These methods focus on training a model from scratch, whereas this paper studies how to fine-tune a model better by shifting tokens.

### 3 Method

#### 3.1 Motivation

**Feature Definition.** [35] explores the internal workings of LLMs by treating the sequence of hidden states as a Chain-of-Embedding (CoE), representing the model's latent thought process. Their analysis reveals distinct patterns in these CoE features when LLMs produced correct versus incorrect answers. Motivated by this work, we pose the question: Can the internal hidden states of a model be leveraged to detect instances of *Cyclical Reasoning*?

Instead of averaging token representations per layer and forming an embedding trajectory from these layer-wise averages [35, 36], we utilize the sequence of token representations from each layer as our embedding trajectory. The embedding trajectory at layer  $l$ , denoted as  $\mathbf{X}^l$ , is formalized as follows:

$$\mathbf{X}^l = \mathbf{x}_0^l \rightarrow \mathbf{x}_1^l \rightarrow \dots \rightarrow \mathbf{x}_{I-1}^l \rightarrow \mathbf{x}_I^l \quad (1)$$

where  $\mathbf{x}_i^l$  denotes the hidden state of the  $i$ -th token after attention in the  $l$ -th layer,  $I$  is the length of the generated sequence. We measure the LLMs' thinking process by using the relative change in

hidden states at each time step.

$$s(\mathbf{x}_{i-1}^l, \mathbf{x}_i^l) = \frac{\|\mathbf{x}_i^l - \mathbf{x}_{i-1}^l\|_2}{\|\mathbf{x}_{i-1}^l\|_2} \quad (2)$$

Then we define the overall relative change of the embedding trajectories, denoted as  $M(\mathbf{X})$ , as the average of the relative changes between every adjacent tokens across all layers. This can be formalized as follows:

$$M(\mathbf{X}) = \frac{1}{L \times I} \sum_{l=1}^L \sum_{i=1}^I s(\mathbf{x}_{i-1}^l, \mathbf{x}_i^l) \quad (3)$$

where  $L$  is the total number of layers in the LLM,  $I$  is the length of the generated sequence.

**Analysis Setup and Findings.** We train two models on a 20k long CoT using LoRA and full fine-tuning, respectively. We evaluate these models on a randomly selected set of 100 questions from the MATH500 [10], with a sampling of eight times, and exclude questions where all eight generated responses exceed the maximum length limit. For the remaining length-exceeded responses, we truncate them to the average length of the normal (non-length-exceeded) responses and remove all repeated text segments. Finally, we calculate the  $M(\mathbf{X})$  values for both the normal and the length-exceeded responses. The results are shown in Figure 2, we can find that the "Exceed" samples tend to exhibit a lower mean relative change compared to the "Normal" samples in both models, as indicated by the lower median and mean (dashed red line) of the "Exceed" box plots. This suggests that when the models engage in *Cyclical Reasoning* (section 4.2 elaborates on the rationale for using the *Length Exceeded Percentage* to measure *Cyclical Reasoning*), the relative change in their adjacent hidden states tends to be less pronounced on average. Furthermore, this paper finds that the full fine-tuned model exhibits a lower proportion of Exceed samples, and concurrently, the  $M(\mathbf{X})$  value across all its generated samples is also higher.

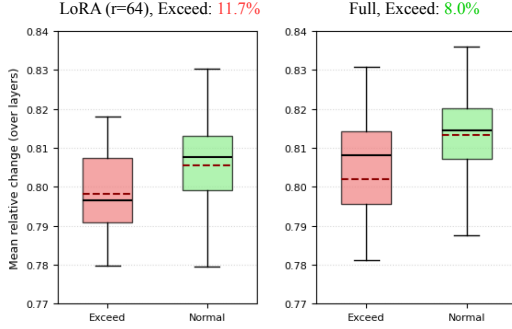


Figure 2: Distribution of the  $M(\mathbf{X})$  for Exceed and Normal samples, comparing LoRA and Full fine-tuned models. The dashed red line represents the mean value.

Based on these findings, a natural research question arises: **Can we mitigate models' *Cyclical Reasoning* issues and consequently enhance its performance by dynamically amplifying representation differences between adjacent tokens?**

### 3.2 Shift Feedforward Network

Motivated by the aforementioned considerations, we propose Shift Feedforward Network (Shift-FFN), an architecture that introduces an Editor module before the FFN. This module uses the preceding token's representation to edit the current token's representation, thereby dynamically amplifying the representation differences between adjacent tokens. The mathematical formulation of this process is as follows:

$$\text{Shift-FFN}(\mathbf{x}_i) = \text{FFN}(\mathbf{x}_i + f_s(\mathbf{x}_{i-1}, \mathbf{x}_i)) \quad (4)$$

where FFN is the original feedforward layer,  $f_s(\cdot)$  represents shift function, which is defined as:

$$f_s(\mathbf{x}_{i-1}, \mathbf{x}_i) = W_c [\text{ReLU}(W_b [\mathbf{x}_{i-1}; \mathbf{x}_i]) \odot (W_a \mathbf{x}_{i-1})] \quad (5)$$

where  $\mathbf{x}_i \in \mathbb{R}^d$  is the representation of token  $i$  after attention,  $[\cdot]$  denotes concatenate operation,  $W_b \in \mathbb{R}^{r \times 2d}$ ,  $W_a \in \mathbb{R}^{r \times d}$  and  $W_c \in \mathbb{R}^{d \times r}$  are parameter matrices in the Editor module, and they are trained from scratch. To maintain a manageable increase in the number of parameters, we set the dimensionality  $r$  to be significantly smaller than  $d$  ( $r \ll d$ ). In LoRA fine-tuning, the value of  $r$  corresponds to the rank of the LoRA. To ensure training stability in the initial stages, we initialize the matrix  $W_c$  as an all-zero matrix. This initialization causes the Shift-FFN to degenerate into the original FFN during the early phase of training.

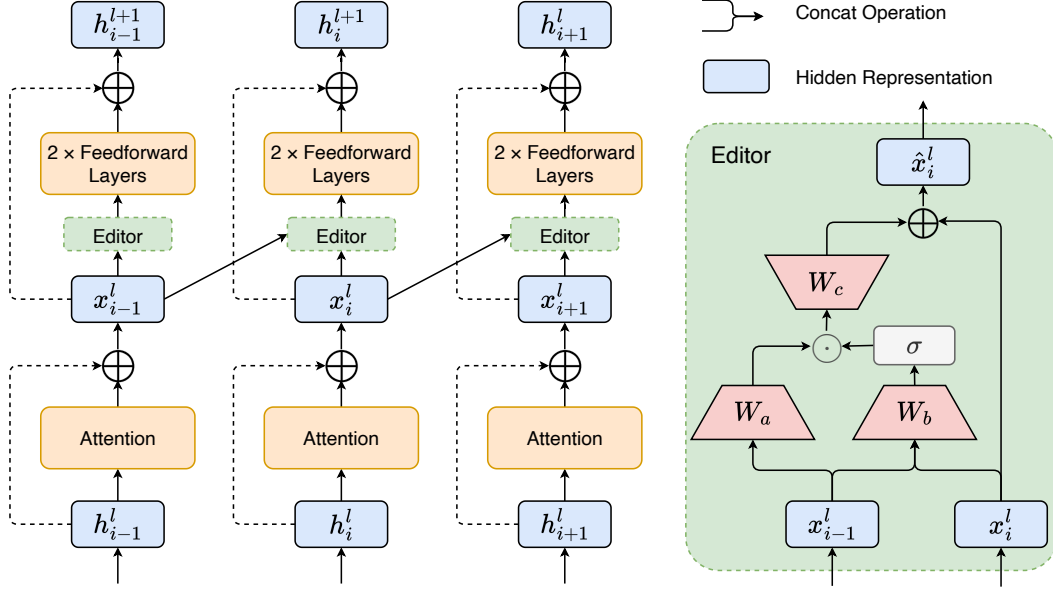


Figure 3: The architecture of Shift-FFN, the **left** side describes the process of shifting token, the **right** side demonstrates the detail of the Editor module.  $\sigma$  is the ReLU function.  $\odot$  and  $\oplus$  are element-wise multiplication and addition, respectively.

### 3.3 Analysis

From simplicity, we consider  $f_s(x_{i-1}, x_i) = W_c W_b x_{i-1} = W_s x_{i-1} = \hat{x}_{i-1}$  and use standard FFN( $x_i$ ) =  $W_{down}[\sigma(W_{up} x_i)]$  in this section.

**From the Perspective of Neural Memory.** [5, 4] proposes that FFN can be regarded as a form of Unnormalized Key-Value Memory [30, 29], where the first linear layer generates the keys, computing a set of retrieval weights for each token. Subsequently, the second linear layer produces the values, which are then multiplied by their corresponding retrieval weights and summed to complete the retrieval process [27]. Therefore, the FFN layer can be also defined as:

$$\text{FFN}(x_i) = \sum_{j=1}^{d_m} w_{i,j} \cdot v_j \quad (6)$$

where  $w_{i,j} = \sigma(x_i^T k_j)$ ,  $k_j$  denotes the  $j$ -th row of  $W_{up}$ ,  $v_j$  denotes the  $j$ -th column of  $W_{down}$ . The  $w_{i,j}$  is the coefficient that assigns weights to the corresponding value vector  $v_j$ . In the scenario of Shift-FFN, the  $w_{i,j}$  is changed as follows:

$$w_{i,j} = \sigma(x_i^T k_j) + \sigma(\hat{x}_{i-1}^T k_j) \quad (7)$$

Therefore, **our Shift-FFN can be viewed as extending the single key retrieval mechanism in Key-Value Memory to a multi-key retrieval in the FFN.** This process is also similar to applying Multi-Query Attention [25] in the FFN.

**From the Perspective of Self Attention.** As defined previously, the output of the Shift-FFN can be expressed as:

$$h_i^{l+1} = W_{down}[\sigma(W_{up}(x_i + \hat{x}_{i-1}))] = h_i + \hat{h}_i \quad (8)$$

where  $h_i$  is the original FFN output,  $\hat{h}_i = W_{down}[\sigma(W_{up}\hat{x}_{i-1})]$  is introduced by Shift-FFN additionally. Then, the attention score  $\alpha_{i,j}$  between token  $i$  and  $j$  at layer  $l+1$  is calculated as follows (residual connections and normalization are omitted):

$$\begin{aligned} \alpha_{i,j} &= [W_q(h_i + \hat{h}_i)]^T [W_k(h_j + \hat{h}_j)] \\ &= \alpha'_{i,j} + (W_q h_i)^T (W_k \hat{h}_j) + (W_q \hat{h}_i)^T (W_k h_j) + (W_q \hat{h}_i)^T (W_k \hat{h}_j) \end{aligned} \quad (9)$$

Table 1: Performance of models on mathematical reasoning benchmarks with different training setups. Each cell presents the *Accuracy* followed by the *Length Exceeded Percentage*  $P_E$  (in parentheses) which indicates the percentage of generated responses exceeding the 32k token limit. The "Param" column indicates the number of trainable parameters. The best performance within each LoRA configuration is highlighted in bold.

	Method	Param	AIME24	AMC23	MATH500	Olympiad	Avg
Qwen2.5-3B	Full	3.09B (100%)	3.1 (80.3)	29.4 (53.2)	51.2 (34.8)	20.2 (55.5)	26.0 (55.9)
	LoRA (r=128)	0.24B (7.8%)	4.3 (62.3)	30.6 (40.1)	54.4 (25.1)	21.9 (41.7)	27.8 (42.3)
	LoRA+Shift-FFN (r=128)	0.28B (9.1%)	<b>4.6</b> (57.1)	<b>31.5</b> (34.7)	<b>55.0</b> (21.2)	<b>23.7</b> (37.0)	<b>28.7</b> (37.5)
	LoRA (r=256)	0.48B (15.6%)	5.4 (49.4)	32.7 (31.6)	57.6 (17.2)	24.1 (31.3)	30.0 (32.3)
	LoRA+Shift-FFN (r=256)	0.55B (18.2%)	<b>7.0</b> (43.2)	<b>35.2</b> (24.9)	<b>60.2</b> (13.9)	<b>25.6</b> (28.2)	<b>32.0</b> (27.5)
Llama3.1-8B	Full	8.03B (100%)	6.7 (23.3)	41.4 (13.5)	63.2 (5.3)	30.7 (12.6)	35.5 (13.7)
	LoRA (r=128)	0.34B (4.2%)	<b>4.6</b> (35.7)	34.0 (22.1)	58.2 (9.3)	26.0 (22.2)	30.7 (22.4)
	LoRA+Shift-FFN (r=128)	0.40B (5.0%)	3.6 (34.5)	<b>34.3</b> (17.6)	<b>60.2</b> (9.0)	<b>27.0</b> (18.3)	<b>31.3</b> (19.8)
	LoRA (r=256)	0.67B (8.4%)	<b>5.4</b> (25.9)	37.8 (15.1)	62.5 (6.6)	29.3 (15.7)	33.7 (15.8)
	LoRA+Shift-FFN (r=256)	0.81B (10.0%)	5.1 (22.8)	<b>38.0</b> (12.1)	<b>63.2</b> (5.1)	<b>29.4</b> (13.7)	<b>34.0</b> (13.4)
Qwen2.5-7B	Full	7.62B (100%)	20.0 (42.3)	58.1 (17.3)	78.7 (8.0)	42.1 (23.6)	49.3 (24.7)
	LoRA (r=128)	0.32B (4.2%)	17.8 (42.5)	54.7 (20.2)	76.1 (8.2)	39.9 (24.1)	47.1 (23.7)
	LoRA+Shift-FFN (r=128)	0.37B (4.9%)	<b>18.2</b> (35.6)	<b>55.6</b> (15.3)	<b>78.1</b> (7.0)	<b>41.0</b> (19.1)	<b>48.2</b> (19.2)
	LoRA (r=256)	0.64B (8.4%)	21.0 (28.6)	58.5 (10.9)	79.1 (5.2)	43.0 (15.2)	50.4 (15.0)
	LoRA+Shift-FFN (r=256)	0.75B (9.8%)	<b>21.8</b> (23.5)	<b>59.1</b> (9.9)	<b>79.9</b> (4.1)	<b>43.8</b> (13.1)	<b>51.2</b> (12.7)

where  $W_q$  and  $W_k$  denote the Query and Key parameter matrices at layer  $l + 1$ ,  $\alpha'_{i,j} = (W_q \mathbf{h}_i)^T (W_k \mathbf{h}_j)$  is the original attention score, and we have

$$(W_q \mathbf{h}_i)^T (W_k \hat{\mathbf{h}}_j) = \mathbf{h}_i^T W_q^T W_k W_{down} [\sigma(W_{up} \hat{\mathbf{x}}_{j-1})] \quad (10)$$

Let  $A_i = \mathbf{h}_i^T W_q^T W_k W_{down}$ . Finally, neglecting the higher-order infinitesimal terms, and substituting  $\hat{\mathbf{x}}_{i-1} = W_s \mathbf{x}_{i-1}$ , we can express  $\alpha_{ij}$  as:

$$\alpha_{i,j} = \alpha'_{i,j} + A_i [\sigma(W_{up} W_s \mathbf{x}_{j-1})] + A_j [\sigma(W_{up} W_s \mathbf{x}_{i-1})] \quad (11)$$

As evident from the derived formulas, the Shift-FFN effectively augments the original attention score with a correction term that is contingent on the  $(i - 1)$ -th and  $(j - 1)$ -th tokens.

## 4 Experiment

### 4.1 Experiment Setup

**Training Data.** To compare the models' performance under short CoT and long CoT conditions, we specifically select the mathematics portion of the OpenThoughts dataset [32], which collects long CoT from DeepSeek-R1 [3]. Our short CoT data is from the Numina-Math dataset [16]. Additionally, we exclude OpenThoughts samples with response lengths exceeding 16k to prevent our models from learning incomplete reasoning processes. After this filtering, we retain a total of 89k training examples, from which we randomly sample 20k for our main experiment.

**Training Setup.** We utilize the LlamaFactory framework [47] and LoRA [12] to fine-tune the Qwen2.5-3B-Instruct, Qwen2.5-7B-Instruct and Llama3.2-8B-Instruct with a batch size of 96 and a learning rate of  $1e-4$ , employing a warm-up ratio of 0.1 and a linear learning rate decay schedule, similar to [15]. For full fine-tuning, we maintain the same hyperparameters except for a learning rate of  $1e-5$ . The max sequence length is set to 16k for all training. All experiments are conducted on  $8 \times 80G$  L20 GPUs.

**Evaluation Setup.** We evaluate our models on four mathematical reasoning datasets: AIME24, AMC23, MATH500 [10], and OlympiadBench [8]. We use a sampling temperature of 0.6 and set the maximum generation length to 32k tokens. To mitigate the impact of randomness in the results, we average over 32 runs for AIME and AMC, and 4 runs for the other tasks.

Table 2: Comparison of models’ performance w.t./w.o. Shift-FFN under comparable trainable parameters. Each cell presents the *Accuracy* followed by the *Length Exceeded Percentage*  $P_E$  (in parentheses) which indicates the percentage of generated responses exceeding the 32k token limit.

Method	Param	AIME24	AMC23	MATH500	Olympiad	Avg
Lora (r=128)	0.32B (4.2%)	17.8 (42.5)	54.7 (20.2)	76.1 (8.2)	39.9 (24.1)	47.1 (23.7)
LoRA (r=148)	0.37B (4.9%)	17.5 (40.9)	55.3 (18.2)	76.8 (8.6)	40.6 (22.1)	47.5 (22.4)
LoRA+Shift-FFN (r=128)	0.37B (4.9%)	<b>18.2</b> (35.6)	<b>55.6</b> (15.3)	<b>78.1</b> (7.0)	<b>41.0</b> (19.1)	<b>48.2</b> (19.2)
LoRA (r=256)	0.64B (8.4%)	21.0 (28.6)	58.5 (10.9)	79.1 (5.2)	43.0 (15.2)	50.4 (15.0)
LoRA (r=296)	0.75B (9.8%)	21.2 (28.4)	58.5 (13.6)	79.3 (6.0)	43.2 (15.5)	50.6 (15.9)
LoRA+Shift-FFN (r=256)	0.75B (9.8%)	<b>21.8</b> (23.5)	<b>59.1</b> (9.9)	<b>79.9</b> (4.1)	<b>43.8</b> (13.1)	<b>51.2</b> (12.7)

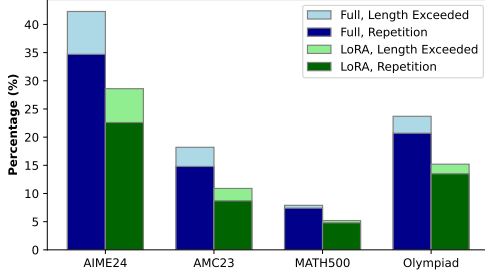


Figure 4: Proportion of length-exceeded and repetition samples in different models.

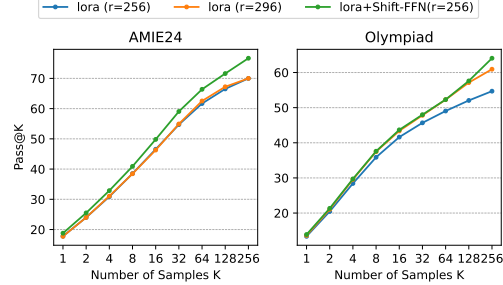


Figure 5: Pass@K of models with different training setups on AIME24 and OlympiadBench.

## 4.2 Main Results

Table 1 presents the results of full fine-tuning and LoRA fine-tuning (with and without Shift-FFN) for various models. The results reveal several findings as follows:

**Long CoT Learning Requires Higher LoRA Rank.** We find that in long CoT scenarios, achieving performance with LoRA comparable to full fine-tuning necessitates a higher LoRA rank, such as 256, in contrast to simpler tasks like common-sense reasoning where a much lower rank (e.g., 32) often suffices to approximate full fine-tuning performance.

**Cyclical Reasoning.** We quantify the *Cyclical Reasoning* by using the *Length Exceeded Percentage* (denoted as  $P_E$ ) – the proportion of generated samples exceeding the 32k token limit. Given the maximum training sequence length of 16k, a 32k limit during inference is ample for generating correct answers; therefore, exceeding this limit is considered indicative of the model getting stuck in a loop. We further analyze the proportion of repetitive output within these length-exceeded samples, where the model repeatedly generates the same segment of text until the maximum limit is reached. The results of this analysis are presented in Figure 4. We find that over 80% of the length-exceeded samples exhibit exact textual repetition. While the remaining 20% do not show identical text repetition, they still demonstrate patterns of *Cyclical Reasoning*, such as repeatedly verifying the same step or iterating through the same few inference steps, concrete examples can be found in Appendix D. Therefore, utilizing the  $P_E$  as a metric for *Cyclical Reasoning* is a justifiable approach. Using this metric, we find that models trained on long CoT data tend to exhibit *Cyclical Reasoning*. Even the full fine-tuned Qwen2.5-7B-Instruct shows a 24.7% *Cyclical Reasoning* ratio. When using LoRA fine-tuning, this ratio decreases as the rank increases. Interestingly, we find that LoRA fine-tuned Qwen2.5-7B-Instruct with a rank of 256 significantly reduces the *Cyclical Reasoning* ratio by 12% compared to full fine-tuning.

**Effectiveness of Shift-FFN.** It can be found that the integration of Shift-FFN consistently yields performance improvements across all settings. Specifically, the Qwen2.5-7B-Instruct model trained with LoRA at rank 256 already achieves an average accuracy 0.9% higher than the full fine-tuned model. Upon introducing Shift-FFN, the model’s average performance further improves by 0.8% to 51.2%, surpassing the full fine-tuned baseline and the original LoRA model across all datasets. Furthermore, Shift-FFN not only enhances performance but also significantly reduces *Cyclical Reasoning*, which is reflected by the decreasing of  $P_E$  from 15.0% to 12.7%.



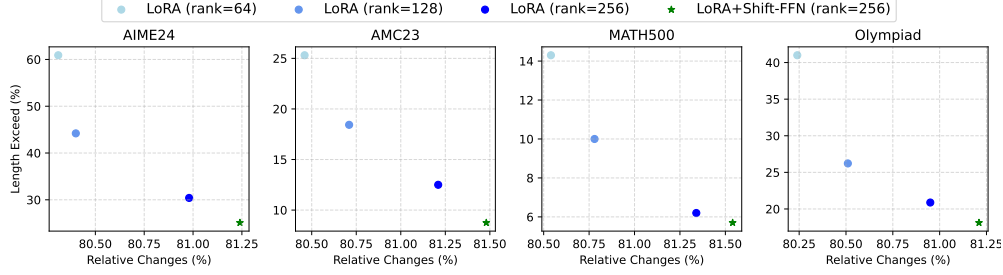


Figure 6: Comparison of *Mean Relative Change*  $M(\mathbf{X})$  and *Length Exceeded Percentage*  $P_E$  for non-length-exceeded samples across models trained with different settings on four datasets.

### 4.3 Compared to LoRA With the Same Number of Parameters

As Shift-FFN introduces extra parameters, to compare it more fairly with standard LoRA, we increase LoRA’s rank (e.g., from 256 to 296) in the training of Qwen2.5-7B-Instruct. This makes the total number of parameters the same as LoRA+Shift-FFN. Table 2 shows the experimental results. It can be found that compared to simply increasing the rank, introducing Shift-FFN brings a larger improvement with a similar number of added parameters. Specifically, when the rank is 256, increasing it to 296 only slightly improves the average performance from 50.4% to 50.6% and also increases the  $P_E$ . However, introducing Shift-FFN raises it to 51.2% and also further reduces the  $P_E$ . A possible explanation is that at a rank of 256, LoRA is nearing its performance limit, so further increasing the rank yields diminishing returns. **However, introducing Shift-FFN can further improve the model’s performance limit from the perspective of representation learning.**

To further validate the effectiveness of Shift-FFN, we evaluate the pass@K metric on the AIME 24 and OlympiadBench datasets. For computational efficiency, we select the first 64 questions from OlympiadBench and set the maximum generation length to 16k. The results of these experiments are presented in Figure 5. It demonstrates that incorporating Shift-FFN leads to improvements across all pass@K metrics. Specifically, on the AIME 24 dataset, pass@256 increases from 70.0% to 76.7% with the addition of Shift-FFN. A potential reason for this is that Shift-FFN reduces the tendency of the model to engage in *Cyclical Reasoning* ( $P_E$  decreases from 28.4% to 23.5%), thereby enhancing the model’s exploration efficiency. On OlympiadBench, the  $P_E$  only decreases by 2.1% with the integration of Shift-FFN. Consequently, the difference in pass@K is not significant for  $K \leq 64$ . The performance gap only becomes more apparent as K increases further. Shift-FFN also consistently achieves the best performance across different sampling temperatures, more details can be found in Appendix C.

### 4.4 Mean Relative Changes with Shift-FFN

To further investigate the relationship between *Mean Relative Change*  $M(\mathbf{X})$  and *Length Exceeded Percentage*  $P_E$ , as well as the impact of Shift-FFN, we analyze these metrics for Qwen2.5-7B-Instruct with different training settings across the datasets, as shown in Figure 6. We find that as the LoRA rank increases, the model’s  $M(\mathbf{X})$  also increases, while  $P_E$  decreases correspondingly. This indicates a negative correlation between  $M(\mathbf{X})$  and  $P_E$ . Specifically, for the AIME24 dataset, when the rank increases from 64 (light blue point) to 256 (dark blue point),  $M(\mathbf{X})$  increases from 80.31% to 80.98%, and  $P_E$  correspondingly decreases from 60.9% to 30.4%. This suggests that as the model has more trainable parameters in the LoRA settings, it becomes less prone to generating *Cyclical Reasoning*, and the relative changes between its internal adjacent tokens become more pronounced. The introduction of Shift-FFN consistently achieves the lowest  $P_E$  and the highest  $M(\mathbf{X})$ . For example, on the AIME24 dataset, introducing Shift-FFN increases  $M(\mathbf{X})$  from 80.98% to 81.24%, and also further reduces  $P_E$  from 30.4% to 25.1%. Furthermore, we find that the higher the original  $P_E$  of the model on a dataset, the greater the benefit brought by introducing Shift-FFN. This indicates that Shift-FFN effectively mitigates the issue of *Cyclical Reasoning* by enabling a dynamic amplifying the representation differences between adjacent tokens.



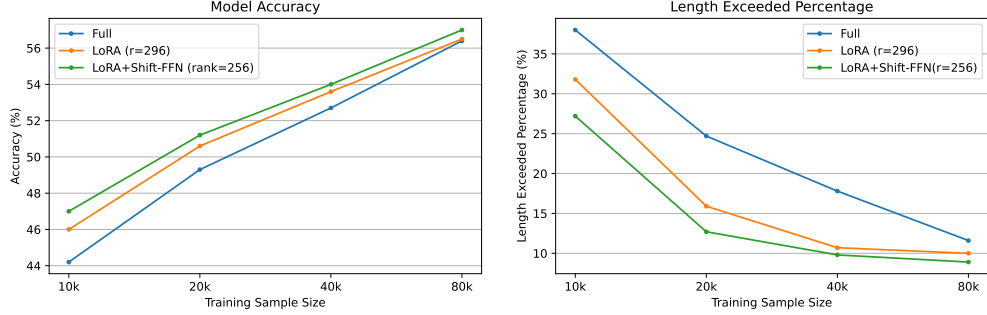


Figure 7: The *Accuracy* (left) and the *Length Exceeded Percentage*  $P_E$  (right) of different fine-tuned models under varying training sample sizes. *Accuracy* and *Length Exceeded Percentage* are the average values obtained on four datasets.

#### 4.5 Performance of Shift-FFN with Varying Training Data Sizes

To evaluate the performance of Shift-FFN with varying training data sizes, we randomly sample 10k, 20k, 40k, and 80k examples from OpenThoughts for training. For each data size, we train three models: Full fine-tuning, LoRA ( $r=296$ ), and LoRA+Shift-FFN ( $r=256$ ). The results are depicted in Figure 7. We notice that as the training sample size increases, the performance of all models improves, and the  $P_E$  decreases. Interestingly, LoRA fine-tuned models consistently outperform the full fine-tuned model across all data scales and are less prone to generating length-exceeded outputs, particularly with smaller training datasets. Specifically, with only 10k training samples, the full fine-tuned model shows a 38.0% of  $P_E$ , while the LoRA fine-tuned model exhibits only 31.9%. This gap narrows as the training data increases to 80k. Furthermore, incorporating Shift-FFN consistently enhances the performance of the original LoRA model across all data sizes. Even with 80k training samples, the LoRA+Shift-FFN model achieves an average accuracy 0.6% higher than the full fine-tuned model and demonstrates superior performance on all datasets. This experiment further illustrates the scalability of Shift-FFN.

#### 4.6 Ablation Studies

Table 3 presents the results of ablation studies, where we evaluate four configurations: (1) w/o  $x_{i-1}$ , which removes the preceding token’s participation in the Editor module,  $f_s = W_c [ReLU(W_b x_i) \odot (W_a x_i)]$ ; (2) w/o  $x_i$  in gate, which only use the  $x_{i-1}$  in the gating mechanism,  $f_s = W_c [ReLU(W_b x_{i-1}) \odot (W_a x_{i-1})]$ ; (3) w/o gate, which disables the gating mechanism,  $f_s = W_c (W_a x_{i-1})$ ; (4) w/o MLP, which directly performs a linear combination of adjacent tokens,  $f_s = \tanh(w^T x_{i-1}) x_{i-1}$ . The experimental results demonstrate that excluding the preceding token leads to performance nearly identical to standard LoRA, indicating that traditional representation learning offers negligible improvement under the LoRA. Furthermore, we find that the gate mechanism that considering both  $x_{i-1}$  and  $x_i$  is crucial in the Editor module. Without it, performance is even lower than standard LoRA. Thus, dynamically editing representations based on adjacent tokens is vital. It can also be found that performing a linear combination of adjacent tokens without applying MLP to the preceding token doesn’t bring any benefit.

Table 3: Ablation Studies on Qwen2.5-7B-Instruct.

	Accuracy ( $\uparrow$ )	Exceed ( $\downarrow$ )
LoRA	50.4	15.0
LoRA+Shift-FFN	<b>51.2</b>	<b>12.7</b>
- w/o $x_{i-1}$	50.2	14.2
- w/o $x_i$ in gate	49.8	13.8
- w/o gate	49.3	14.3
- w/o MLP	50.3	17.0

## 5 Conclusion

This work finds that fine-tuning LLMs with full parameters or LoRA with a low rank on long CoT data often leads to *Cyclical Reasoning*, where models repeatedly reiterate previous inference steps until the maximum length limit. Investigating the models’ internal states, this paper finds that *Cyclical Reasoning* is more likely when the representation differences between adjacent tokens are small.

To address this, we propose Shift-FFN, an architecture that introduces an Editor module before the FFN. This module uses the preceding token’s representation to edit the current token’s representation, thereby dynamically amplifying the representation differences between adjacent tokens. Experimental results demonstrate that LoRA combined with Shift-FFN achieves higher accuracy and a lower rate of *Cyclical Reasoning* across various data sizes compared to full fine-tuning and standard LoRA.

## References

- [1] Qiguang Chen, Libo Qin, Jinhao Liu, Dengyun Peng, Jiannan Guan, Peng Wang, Mengkang Hu, Yuhang Zhou, Te Gao, and Wanxiang Che. Towards Reasoning Era: A Survey of Long Chain-of-Thought for Reasoning Large Language Models, April 2025. arXiv:2503.09567 [cs].
- [2] Christopher Clark, Kenton Lee, Ming-Wei Chang, Tom Kwiatkowski, Michael Collins, and Kristina Toutanova. Boolq: Exploring the surprising difficulty of natural yes/no questions. *arXiv preprint arXiv:1905.10044*, 2019.
- [3] DeepSeek-AI, Daya Guo, Dejian Yang, Haowei Zhang, Junxiao Song, Ruoyu Zhang, Runxin Xu, Qihao Zhu, Shirong Ma, Peiyi Wang, Xiao Bi, et al. DeepSeek-R1: Incentivizing Reasoning Capability in LLMs via Reinforcement Learning, January 2025. arXiv:2501.12948 [cs].
- [4] Mor Geva, Avi Caciularu, Kevin Ro Wang, and Yoav Goldberg. Transformer feed-forward layers build predictions by promoting concepts in the vocabulary space. *arXiv preprint arXiv:2203.14680*, 2022.
- [5] Mor Geva, Roei Schuster, Jonathan Berant, and Omer Levy. Transformer Feed-Forward Layers Are Key-Value Memories. In *Proceedings of the 2021 Conference on Empirical Methods in Natural Language Processing*, pages 5484–5495, Online and Punta Cana, Dominican Republic, November 2021. Association for Computational Linguistics.
- [6] Aaron Grattafiori, Abhimanyu Dubey, Abhinav Jauhri, Abhinav Pandey, Abhishek Kadian, Ahmad Al-Dahle, Aiesha Letman, Akhil Mathur, Alan Schelten, Alex Vaughan, et al. The llama 3 herd of models. *arXiv preprint arXiv:2407.21783*, 2024.
- [7] Zeyu Han, Chao Gao, Jinyang Liu, Jeff Zhang, and Sai Qian Zhang. Parameter-Efficient Fine-Tuning for Large Models: A Comprehensive Survey, September 2024. arXiv:2403.14608 [cs].
- [8] Chaoqun He, Renjie Luo, Yuzhuo Bai, Shengding Hu, Zhen Leng Thai, Junhao Shen, Jinyi Hu, Xu Han, Yujie Huang, Yuxiang Zhang, et al. Olympiadbench: A challenging benchmark for promoting agi with olympiad-level bilingual multimodal scientific problems. *arXiv preprint arXiv:2402.14008*, 2024.
- [9] Shwai He, Liang Ding, Daize Dong, Miao Zhang, and Dacheng Tao. Sparseadapter: An easy approach for improving the parameter-efficiency of adapters. *arXiv preprint arXiv:2210.04284*, 2022.
- [10] Dan Hendrycks, Collin Burns, Saurav Kadavath, Akul Arora, Steven Basart, Eric Tang, Dawn Song, and Jacob Steinhardt. Measuring mathematical problem solving with the math dataset. *arXiv preprint arXiv:2103.03874*, 2021.
- [11] Neil Houlsby, Andrei Giurgiu, Stanislaw Jastrzebski, Bruna Morrone, Quentin De Laroussilhe, Andrea Gesmundo, Mona Attariyan, and Sylvain Gelly. Parameter-efficient transfer learning for nlp. In *International conference on machine learning*, pages 2790–2799. PMLR, 2019.
- [12] Edward J. Hu, Yelong Shen, Phillip Wallis, Zeyuan Allen-Zhu, Yanzhi Li, Shean Wang, Lu Wang, and Weizhu Chen. LoRA: Low-Rank Adaptation of Large Language Models, October 2021. arXiv:2106.09685 [cs].
- [13] Aaron Jaech, Adam Kalai, Adam Lerer, Adam Richardson, Ahmed El-Kishky, Aiden Low, Alec Helyar, Aleksander Madry, Alex Beutel, Alex Carney, et al. Openai o1 system card. *arXiv preprint arXiv:2412.16720*, 2024.

- [14] Brian Lester, Rami Al-Rfou, and Noah Constant. The power of scale for parameter-efficient prompt tuning. *arXiv preprint arXiv:2104.08691*, 2021.
- [15] Dacheng Li, Shiyi Cao, Tyler Griggs, Shu Liu, Xiangxi Mo, Shishir G. Patil, Matei Zaharia, Joseph E. Gonzalez, and Ion Stoica. LLMs Can Easily Learn to Reason from Demonstrations Structure, not content, is what matters!, February 2025. *arXiv:2502.07374* [cs].
- [16] Jia LI, Edward Beeching, Lewis Tunstall, Ben Lipkin, Roman Soletskyi, Shengyi Costa Huang, Kashif Rasul, Longhui Yu, Albert Jiang, Ziju Shen, Zihan Qin, Bin Dong, Li Zhou, Yann Fleureau, Guillaume Lample, and Stanislas Polu. NuminaMath. [<https://huggingface.co/AI-MO/NuminaMath-CoT>] ([https://github.com/project-numina/aimo-progress-prize/blob/main/report/numina\\_dataset.pdf](https://github.com/project-numina/aimo-progress-prize/blob/main/report/numina_dataset.pdf)), 2024.
- [17] Xiang Lisa Li and Percy Liang. Prefix-Tuning: Optimizing Continuous Prompts for Generation, January 2021. *arXiv:2101.00190* [cs].
- [18] Xuechen Li, Tianyi Zhang, Yann Dubois, Rohan Taori, Ishaan Gulrajani, Carlos Guestrin, Percy Liang, and Tatsunori B Hashimoto. AlpacaEval: An automatic evaluator of instruction-following models, 2023.
- [19] Zhixuan Lin, Evgenii Nikishin, Xu Owen He, and Aaron Courville. Forgetting Transformer: Softmax Attention with a Forget Gate, March 2025. *arXiv:2503.02130* [cs].
- [20] Sheng Liu, Haotian Ye, Lei Xing, and James Zou. In-context vectors: Making in context learning more effective and controllable through latent space steering. *arXiv preprint arXiv:2311.06668*, 2023.
- [21] Weiyang Liu, Zeju Qiu, Yao Feng, Yuliang Xiu, Yuxuan Xue, Longhui Yu, Haiwen Feng, Zhen Liu, Juyeon Heo, Songyou Peng, et al. Parameter-efficient orthogonal finetuning via butterfly factorization. *arXiv preprint arXiv:2311.06243*, 2023.
- [22] Wenhao Liu, Xiaohua Wang, Muling Wu, Tianlong Li, Changze Lv, Zixuan Ling, Jianhao Zhu, Cenyuan Zhang, Xiaoqing Zheng, and Xuanjing Huang. Aligning large language models with human preferences through representation engineering. *arXiv preprint arXiv:2312.15997*, 2023.
- [23] Yijia Luo, Yulin Song, Xingyao Zhang, Jiaheng Liu, Weixun Wang, GengRu Chen, Wenbo Su, and Bo Zheng. Deconstructing Long Chain-of-Thought: A Structured Reasoning Optimization Framework for Long CoT Distillation, March 2025. *arXiv:2503.16385* [cs].
- [24] Bo Peng, Eric Alcaide, Quentin Anthony, Alon Albalak, Samuel Arcadinho, Stella Biderman, Huanqi Cao, Xin Cheng, Michael Chung, Matteo Grella, et al. RwkV: Reinventing rnnns for the transformer era. *arXiv preprint arXiv:2305.13048*, 2023.
- [25] Noam Shazeer. Fast transformer decoding: One write-head is all you need. *arXiv preprint arXiv:1911.02150*, 2019.
- [26] Noam Shazeer. Glu variants improve transformer. *arXiv preprint arXiv:2002.05202*, 2020.
- [27] Ying Shen and Lifu Huang. LLM Braces: Straightening Out LLM Predictions with Relevant Sub-Updates, March 2025. *arXiv:2503.16334* [cs].
- [28] Nishant Subramani, Nivedita Suresh, and Matthew E Peters. Extracting latent steering vectors from pretrained language models. *arXiv preprint arXiv:2205.05124*, 2022.
- [29] Sainbayar Sukhbaatar, Edouard Grave, Guillaume Lample, Herve Jegou, and Armand Joulin. Augmenting self-attention with persistent memory. *arXiv preprint arXiv:1907.01470*, 2019.
- [30] Sainbayar Sukhbaatar, Jason Weston, Rob Fergus, et al. End-to-end memory networks. *Advances in neural information processing systems*, 28, 2015.
- [31] Xinyu Tang, Xiaolei Wang, Zhihao Lv, Yingqian Min, Wayne Xin Zhao, Binbin Hu, Ziqi Liu, and Zhiqiang Zhang. Unlocking General Long Chain-of-Thought Reasoning Capabilities of Large Language Models via Representation Engineering, March 2025. *arXiv:2503.11314* [cs].

- [32] OpenThoughts Team. Open Thoughts. <https://open-thoughts.ai>, January 2025.
- [33] Ashish Vaswani, Noam Shazeer, Niki Parmar, Jakob Uszkoreit, Llion Jones, Aidan N. Gomez, Lukasz Kaiser, and Illia Polosukhin. Attention Is All You Need, December 2017. arXiv:1706.03762 [cs].
- [34] Yaqing Wang, Sahaj Agarwal, Subhabrata Mukherjee, Xiaodong Liu, Jing Gao, Ahmed Hassan Awadallah, and Jianfeng Gao. Adamix: Mixture-of-adaptations for parameter-efficient model tuning. *arXiv preprint arXiv:2205.12410*, 2022.
- [35] Yiming Wang, Pei Zhang, Baosong Yang, Derek F. Wong, and Rui Wang. Latent Space Chain-of-Embedding Enables Output-free LLM Self-Evaluation, March 2025. arXiv:2410.13640 [cs].
- [36] Yiming Wang, Pei Zhang, Baosong Yang, Derek F. Wong, Zhuosheng Zhang, and Rui Wang. Embedding Trajectory for Out-of-Distribution Detection in Mathematical Reasoning, October 2024. arXiv:2405.14039 [cs].
- [37] Jason Wei, Xuezhi Wang, Dale Schuurmans, Maarten Bosma, Brian Ichter, Fei Xia, Ed Chi, Quoc Le, and Denny Zhou. Chain-of-Thought Prompting Elicits Reasoning in Large Language Models, January 2023. arXiv:2201.11903 [cs].
- [38] Liang Wen, Yunke Cai, Fenrui Xiao, Xin He, Qi An, Zhenyu Duan, Yimin Du, Junchen Liu, Lifu Tang, Xiaowei Lv, Haosheng Zou, Yongchao Deng, Shousheng Jia, and Xiangzheng Zhang. Light-rl: Curriculum sft, dpo and rl for long cot from scratch and beyond. *arXiv preprint arXiv:2503.10460*, 2025.
- [39] Muling Wu, Wenhao Liu, Xiaohua Wang, Tianlong Li, Changze Lv, Zixuan Ling, Jianhao Zhu, Cenyuan Zhang, Xiaoqing Zheng, and Xuanjing Huang. Advancing Parameter Efficiency in Fine-tuning via Representation Editing, June 2024. arXiv:2402.15179 [cs].
- [40] Zhengxuan Wu, Aryaman Arora, Zheng Wang, Atticus Geiger, Dan Jurafsky, Christopher D. Manning, and Christopher Potts. ReFT: Representation Finetuning for Language Models, May 2024. arXiv:2404.03592 [cs].
- [41] Mingyu Xu, Wei Cheng, Bingning Wang, and Weipeng Chen. KV Shifting Attention Enhances Language Modeling, December 2024. arXiv:2411.19574 [cs].
- [42] Xiaohan Xu, Ming Li, Chongyang Tao, Tao Shen, Reynold Cheng, Jinyang Li, Can Xu, Dacheng Tao, and Tianyi Zhou. A survey on knowledge distillation of large language models. *arXiv preprint arXiv:2402.13116*, 2024.
- [43] An Yang, Baosong Yang, Beichen Zhang, Binyuan Hui, Bo Zheng, Bowen Yu, Chengyuan Li, Dayiheng Liu, Fei Huang, Haoran Wei, Huan Lin, Jian Yang, Jianhong Tu, Jianwei Zhang, Jianxin Yang, Jiaxi Yang, Jingren Zhou, Junyang Lin, Kai Dang, Keming Lu, Keqin Bao, Kexin Yang, Le Yu, Mei Li, Mingfeng Xue, Pei Zhang, Qin Zhu, Rui Men, Runji Lin, Tianhao Li, Tingyu Xia, Xingzhang Ren, Xuancheng Ren, Yang Fan, Yang Su, Yichang Zhang, Yu Wan, Yuqiong Liu, Zeyu Cui, Zhenru Zhang, and Zihan Qiu. Qwen2.5 technical report. *arXiv preprint arXiv:2412.15115*, 2024.
- [44] Yixin Ye, Zhen Huang, Yang Xiao, Ethan Chern, Shijie Xia, and Pengfei Liu. LIMO: Less is More for Reasoning, February 2025. arXiv:2502.03387 [cs].
- [45] Biao Zhang and Rico Sennrich. Root mean square layer normalization. *Advances in Neural Information Processing Systems*, 32, 2019.
- [46] Qingru Zhang, Minshuo Chen, Alexander Bukharin, Nikos Karampatziakis, Pengcheng He, Yu Cheng, Weizhu Chen, and Tuo Zhao. AdaLoRA: Adaptive Budget Allocation for Parameter-Efficient Fine-Tuning, December 2023. arXiv:2303.10512 [cs].
- [47] Yaowei Zheng, Richong Zhang, Junhao Zhang, Yanhan Ye, Zheyang Luo, Zhangchi Feng, and Yongqiang Ma. Llamafactory: Unified efficient fine-tuning of 100+ language models. *arXiv preprint arXiv:2403.13372*, 2024.

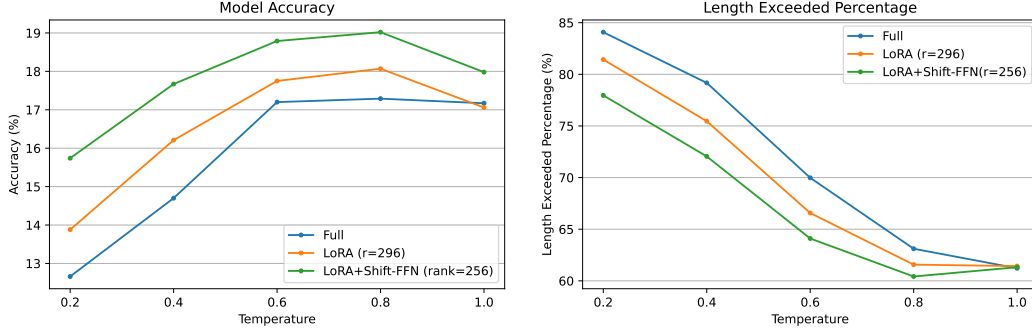


Figure 8: The *Accuracy* (left) and the *Length Exceeded Percentage* (right) of different fine-tuned models for under varying sampling temperatures on AIME24.

## A Limitation

Our study has two main limitations: (1) Due to resource constraints, we do not conduct experiments with larger datasets (e.g., 1M) or models (e.g., 32B), so the scalability of Shift-FFN remains an open question. (2) We only observe that the smaller the difference between adjacent tokens, the more prone the model is to cyclical reasoning. However, we do not conduct further analysis into the deeper reasons behind this phenomenon.

## B Feedforward Network

A Transformer language model [33] consists of layers of multi-head self-attention (MHSA) and position-wise feedforward networks (FFN). Each feedforward layer operates independently on individual position vectors in the sequence. The standard FFN can be expressed as follows (bias terms are omitted):

$$\text{FFN}(\mathbf{x}_i) = W_{\text{down}}[\sigma(W_{\text{up}} \mathbf{x}_i)] \quad (12)$$

where  $W_{\text{down}} \in \mathbb{R}^{d_m \times d}$  and  $W_{\text{up}} \in \mathbb{R}^{d \times d_m}$  are parameter matrices,  $\mathbf{x}_i \in \mathbb{R}^d$  is the representation of token  $i$  after MHSA and  $\sigma$  represents a nonlinear activation function.

An alternative to the standard FFN is the Gated Linear Unit [26] variant, which has shown improved performance in some scenarios. The GLU-FFN is defined as (bias terms are omitted):

$$\text{FFN}_{\text{GLU}}(\mathbf{x}_i) = W_{\text{down}}(\sigma(W_{\text{gate}} \mathbf{x}_i) \odot (W_{\text{up}} \mathbf{x}_i)) \quad (13)$$

where  $\odot$  denotes element-wise multiplication, and  $W_{\text{gate}}, W_{\text{up}} \in \mathbb{R}^{d \times d_m}$ ,  $W_{\text{down}} \in \mathbb{R}^{d_m \times d}$  are parameter matrices. This gating mechanism allows for more flexible information flow and has better performance [26]. Contemporary models such as LLaMA [6] and Qwen [43] predominantly employ GLU-FFN. Our Shift-FFN can be applied to any type of FFN.

## C Performance under Varying Sampling Temperatures

We also further investigate the impact of sampling temperature on model performance and the rate of *Cyclical Reasoning*. Specifically, we examine the performance of Qwen2.5-7B-Instruct, fine-tuned with different strategies, at sampling temperatures of 0.2, 0.4, 0.6, 0.8, and 1.0. The maximum generation length is set to 16k for computational efficiency. The experimental results are shown in Figure 8. We observe that at lower sampling temperatures, the models exhibit not only lower accuracy but also a higher *Length Exceeded Percentage*, indicating a greater tendency for *Cyclical Reasoning*. The overall performance of the models appears optimal within the sampling temperature range of 0.6 to 0.8; further increases beyond this range tend to result in a decline in performance. Notably, LoRA+Shift-FFN (r=256) consistently achieves the highest accuracy across all tested sampling temperatures. Based on Figure 9, we also investigate the Pass@K performance of the models at different sampling temperatures. The trend in Pass@K values aligns with the average accuracy observed earlier, with peak performance generally occurring at a temperature of 0.6. In the

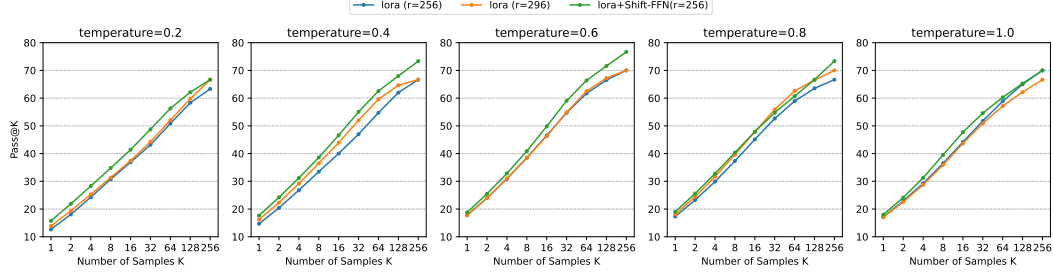


Figure 9: The Pass@K of different fine-tuned models for under varying sampling temperatures on AIME24.

temperature range of 0.2 to 0.6, LoRA+Shift-FFN ( $r=256$ ) exhibits a clear advantage in Pass@K. However, this advantage diminishes at higher sampling temperatures (0.8 and 1.0). A potential explanation for this reduction is that the difference in *Length Exceeded Percentage* between the models decreases at these higher temperatures, leading to similar exploration efficiency. Nevertheless, at the optimal sampling temperature of 0.6, LoRA+Shift-FFN ( $r=256$ ) still demonstrates a significant improvement in Pass@K, validating the effectiveness of our proposed method.

## D Cyclical Reasoning Examples

Table 4 and 5 show examples of *Cyclical Reasoning* in full fine-tuned Qwen2.5-7B-Instruct on AIME24 and MATH500, alongside correct answers generated by the model with Shift-FFN. It can be found that these problems can actually be solved after generating around 10k tokens, but if the model falls into *Cyclical Reasoning*, it will keep generating tokens until it reaches the 32k length limit, which not only reduces the average accuracy but also seriously affects the reasoning efficiency.

Table 4: Generation comparison of Qwen2.5-7B-Instruct under full and LoRA fine-tuning, where the full fine-tuned model shows *Cyclical Reasoning*.

Instruction (AIME24)	Find the largest possible real part of $(75+117i)z + \frac{96+144i}{z}$ where $z$ is a complex number with $ z  = 4$ .
Full	<p>&lt; begin_of_thought &gt;\n\nOkay, so I need to find the largest possible real part of the expression <math>[(75+117i)z + \frac{96+144i}{z}]</math> where <math>(z)</math> is a complex number with <math>( z  = 4)</math>. Hmm, let's start by understanding what the problem is asking.</p> <p>...</p> <p>Therefore, the correct answer is 540.\n\nBut according to the Lagrange multiplier method, it's 518.4. Therefore, there's a contradiction.\n\nThis suggests that the Cauchy-Schwarz approach is incorrect.</p> <p>...</p> <p>Therefore, the correct answer is 540.\n\nBut according to the Lagrange multiplier method, it's 518.4. Therefore, there's a contradiction.\n\nThis suggests that the Cauchy-Schwarz approach is incorrect.</p> <p>...</p> <p>Therefore, the correct answer is 540.\n\nBut according</p> <p>Generation Length: 32768 Result: <b>Wrong (Reaching the maximum length limit)</b></p>
LoRA+Shift-FFN (rank=256)	<p>&lt; begin_of_thought &gt;\n\nOkay, so I need to find the largest possible real part of the expression <math>(75 + 117i)z + (96 + 144i)/z</math>, where <math>z</math> is a complex number with <math> z  = 4</math>. Hmm, let's see. First, I remember that when dealing with complex numbers,</p> <p>...</p> <p>Expanding and combining like terms, this paper finds the real part of the expression:\n\n<math>324\cos\theta - 432\sin\theta</math>\n\nThis real part can be written in the form <math>C\cos(\theta + \phi)</math>, where <math>C = \sqrt{324^2 + (-432)^2} = 540</math>. The maximum value of this expression is therefore <math>540</math>. To verify, we check specific values of <math>(\theta)</math> that align the coefficients with the vector <math>(324, -432)</math>. This confirms that the maximum real part is indeed <math>540</math>. Thus, the largest possible real part is <math>\boxed{540}</math>.</p> <p>&lt; end_of_solution &gt;</p> <p>Generation Length: 9902 Result: <b>Correct</b></p>



Table 5: Generation comparison of Qwen2.5-7B-Instruct under full and LoRA fine-tuning, where the full fine-tuned model shows *Cyclical Reasoning*.

<b>Instruction</b> <b>(MATH500)</b>	The expression $2 \cdot 3 \cdot 4 \cdot 5 + 1$ is equal to 121, since multiplication is carried out before addition. However, we can obtain values other than 121 for this expression if we are allowed to change it by inserting parentheses. For example, we can obtain 144 by writing $(2 \cdot (3 \cdot 4)) \cdot (5 + 1) = 144$ . In total, how many values can be obtained from the expression $2 \cdot 3 \cdot 4 \cdot 5 + 1$ by inserting parentheses? (Note that rearranging terms is not allowed, only inserting parentheses).
Full	<p>&lt; begin_of_thoughtl&gt;\n\nOkay, so I need to figure out how many different values can be obtained from the expression <math>2 \cdot 3 \cdot 4 \cdot 5 + 1</math> by inserting parentheses. The key here is that changing the grouping with parentheses can alter the order of operations, which might lead to different results. Let me start by recalling the original expression and how parentheses can affect the calculation.</p> <p>...</p> <p>Wait, no, they are the same. Wait, <math>2 \cdot (3 \cdot 4 \cdot 5) = 2 \cdot 60 = 120</math>, same as <math>(2 \cdot 3) \cdot 4 \cdot 5 = 6 \cdot 20 = 120</math>. So different groupings can lead to the same product.\n\nBut inserting parentheses around different parts can lead to different products. For example, <math>2 \cdot (3 \cdot 4 \cdot 5) = 120</math>, but <math>(2 \cdot 3) \cdot (4 \cdot 5) = 120</math>, but <math>2 \cdot (3 \cdot 4 \cdot 5)</math> is different.</p> <p>Wait, no, they are the same. Wait, <math>2 \cdot (3 \cdot 4 \cdot 5) = 2 \cdot 60 = 120</math>, same as <math>(2 \cdot 3) \cdot 4 \cdot 5 = 6 \cdot 20 = 120</math>. So different groupings can lead to the same product.\n\nBut inserting parentheses around different parts can lead to different products. For example, <math>2 \cdot (3 \cdot 4 \cdot 5) = 120</math>, but <math>(2 \cdot 3) \cdot (4 \cdot 5) = 120</math>, but <math>2 \cdot (3 \cdot 4 \cdot 5)</math> is different. Wait, no, they are the same. Wait, 2</p> <p>Generation Length: 32768 Result: <b>Wrong (Reaching the maximum length limit)</b></p>
LoRA+Shift-FFN (rank=256)	<p>&lt; begin_of_thoughtl&gt;\n\nOkay, so I need to figure out how many different values can be obtained from the expression <math>2 \times 3 \times 4 \times 5 + 1</math> by inserting parentheses. The problem says that rearranging terms isn't allowed, so we have to keep the original order but group the operations differently with parentheses.</p> <p>...</p> <p>*7. <math>(2 \cdot 3 \cdot 4 \cdot 5) + 1</math>**: \n \[ \n 120 + 1 = 121. \n \] \n - **8. <math>(2 \cdot (3 \cdot (4 \cdot 5))) + 1</math>**: \n \[ \n 2 \cdot (120) + 1 = 241. \n \] \n - **9. <math>(2 \cdot 3 \cdot 4) + (5 \cdot 1)</math>**: \n \[ \n 24 + 5 = 29. \n \] \n - **10. <math>(2 \cdot 3) \cdot (4 \cdot (5 + 1))</math>**: \n \[ \n 6 \cdot (4 \cdot 6) = 6 \cdot 24 = 144. \n \] \n - **11. <math>(2 \cdot (3 \cdot 4)) \cdot (5 + 1)</math>**: \n \[ \n 24 \cdot 6 = 144. \n \] \n - **12. <math>2 \cdot ((3 \cdot 4) \cdot (5 + 1))</math>**: \n \[ \n 2 \cdot (12 \cdot 6) = 2 \cdot 72 = 144. \n \] \n 3.</p> <p>**Distinct Values**: \n The distinct results from the valid parenthesizations are: \n - <math>(121)</math>, \n - <math>(241)</math>, \n - <math>(29)</math>, \n - <math>(144)</math>. \n \n Thus, the total number of distinct values obtainable is <math>\boxed{4}</math>. \n \n &lt; end_of_solutionl&gt;</p> <p>Generation Length: 11053 Result: <b>Correct</b></p>